frontiers in Chemistry

ORIGINAL RESEARCH
published: 15 February 2022
doi: 10.3389/fchem.2022.842405

Metabolites With Cytotoxic Activities From the Mangrove Endophytic Fungus *Fusarium* sp. 2ST2

Yan Chen[1,2], Guisheng Wang[1], Yilin Yuan[1], Ge Zou[2], Wencong Yang[2], Qi Tan[2], Wenyi Kang[1] and Zhigang She[2]**

[1]National R & D Center for Edible Fungus Processing Technology, Henan University, Kaifeng, China, [2]School of Chemistry, Sun Yat-sen University, Guangzhou, China

Two new 3-decalinoyltetramic acid derivatives with peroxide bridge fusarisetins E (**1**) and F (**2**), one new chromone fusarimone A (**5**), two new benzofurans fusarifurans A (**9**) and B (**10**), three new isocoumarins fusarimarins A–C (**11–13**), as well as five known analogues **3**, **4**, **6–8** and **14** were isolated from mangrove endophytic fungus *Fusarium* sp. 2ST2. Their structures and absolute configurations were established by spectroscopic analysis, density functional theory-gauge invariant atomic orbital NMR calculation with DP4+ statistical analysis, and electronic circular dichroism calculation. Compounds **1** and **2** showed significant cytotoxicity against human A549 cell lines with IC_{50} values of 8.7 and 4.3 μM, respectively.

Keywords: mangrove, endophytic fungus, *Fusarium* sp., cytotoxicity, benzofuran, chromone

OPEN ACCESS

Edited by:
Xiachang Wang, Nanjing University of Chinese Medicine, China

Reviewed by:
Wei Xu, State Oceanic Administration, China
ChunLan Xie, Xiamen University, China

****Correspondence:***
Wenyi Kang
kangwenyi@henu.edu.cn
Zhigang She
cesshzhg@mail.sysu.edu.cn

Specialty section:
This article was submitted to Organic Chemistry, a section of the journal Frontiers in Chemistry

Received: *23 December 2021*
Accepted: *12 January 2022*
Published: *15 February 2022*

Citation:
Chen Y, Wang G, Yuan Y, Zou G, Yang W, Tan Q, Kang W and She Z (2022) Metabolites With Cytotoxic Activities From the Mangrove Endophytic Fungus Fusarium sp. 2ST2. Front. Chem. 10:842405. doi: 10.3389/fchem.2022.842405

INTRODUCTION

Endophytic fungi, inhabiting plants without any negative effects for the host, have been proven to be a promising source of novel structures and unique bioactivities (Liu et al., 2021; Viridiana et al., 2021). *Fusarium* spp. are endophytic fungi widely distributed in association with plants. It has attracted much attention due to their diverse bioactive secondary metabolites, including alkaloids, terpenes, cyclopeptide, anthraquinone, and lactones (Chen et al., 2019)—for example, indole alkaloids fusaindoterpenes A and B from *Fusarium* sp. showed antiviral activity (Guo et al., 2020), and fusarithioamide A from *Fusarium chlamydosporium* exhibited cytotoxic activity (Ibrahim et al., 2018).

Mangrove endophytic fungi, the second largest ecological group of marine fungi, have been reported to produce thousands of new metabolites until now (Chen et al., 2021; Chen et al., 2022). Over the past 2 decades, our group continues to explore bioactive novel structures from mangrove endophytic fungi (Huang et al., 2013; Xiao et al., 2013; Liu et al., 2016; Cui et al., 2017; Cai et al., 2019). In the course of our ongoing search for new antitumor active compounds from mangrove endophytic fungi, the strain *Fusarium* sp. 2ST2 attracted our attention because of the cytotoxicity of the crude extract. Then, eight new metabolites, including two alkaloids fusarisetin E (**1**) and F (**2**), one chromone fusarimone A (**5**), two benzofurans fusarifurans A (**9**) and B (**10**), three isocoumarins fusarimarins A–C (**11–13**), were obtained together with five analogues equisetin (**3**), epi-equisetin (**4**), takanechromone B (**6**), altechromone A (**7**), 4H-1-benzopyran-4-one-2,3-dihydro-5-hydroxy-8-(hydroxylmethyl)-2-methyl (**8**), and aspergisocoumrin A (**14**) (**Figure 1**). As expected, compounds **1** and **2** exhibited significant cytotoxicity against human A549 cell line, and compounds **8** and **14** showed potent cytotoxicity against A549 and MDA-MB-435 cell lines. The isolation, structure elucidation, and biological evaluation of these compounds were reported herein.

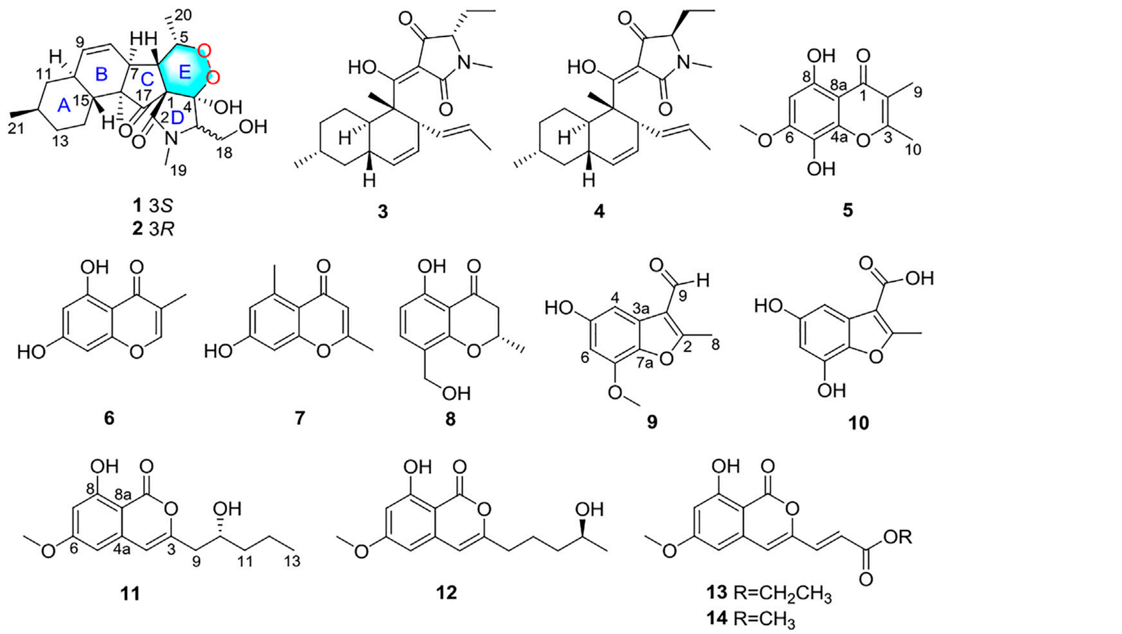

FIGURE 1 | Structures of compounds **1–14**.

MATERIALS AND METHODS

General Experimental Procedures

Optical rotations were measured on a PerkinElmer 341 instrument at 25°C. Melting points were recorded on a Fisher-Johns hot-stage apparatus. UV spectra were measured in MeOH using a Shimadzu UV-2700 spectrophotometer. Electronic circular dichroism (ECD) data were obtained on a Chirascan CD spectrometer (Applied Photophysics). A Bruker Avance 500 spectrometer (^{1}H 500 MHz, ^{13}C 125 MHz) was used for the 1D and 2D NMR data collection. All high-resolution electrospray ionization mass spectrometry (HRESIMS) data were obtained on an Agilent G6230 Q-TOF mass spectrometer. Silica gel (200–300 mesh, Qingdao Marine Chemical Factory) and Sephadex LH-20 (Amersham Pharmacia) were used in the column chromatography (CC). Silica gel plates (Qingdao Huang Hai Chemical Group Co., G60, F-254) were used for the thin-layer chromatography.

Fungal Material

The fungus *Fusarium* sp. 2ST2 was isolated from healthy leaves of *Kandelia candel*, which was collected in June 2015 from the South China Sea, Dong Zhai Harbor Mangrove Nature Reserve Area, Hainan Province, China. The strain was identified as *Fusarium* sp. (GenBank no. MZ801734) by a BLAST search which showed it to be 100% identical with the sequence of *Fusarium* sp. (GenBank no. KU296944.1).

Fermentation, Extraction, and Isolation

The fungus *Fusarium* sp. 2ST2 was cultivated on potato dextrose agar for 5 days. The mycelia of the strain were inoculated into 500 ml potato dextrose broth for 3 days to prepare the seed culture and then inoculated into the solid rice medium (70 g of rice, 3 g peptone, and 50 ml of distilled water, 60 flasks). It was incubated for 30 days at room temperature.

The medium was extracted with MeOH for three times, and the total residue of the strain (65.0 g) was obtained. The EtOAc extract was chromatographed by silica gel CC (200–300 mesh silica) and eluted with an increasing gradient of petroleum ether/EtOAc (9:1 to 1:9) to afford six fractions (Fr. A–F). Fraction B was applied to Sephadex LH-20 CC (CH_2Cl_2/MeOH v/v, 1:1) to give three fractions (Fr. B1–B3). Fraction B1 was subjected to silica gel CC (CH_2Cl_2/MeOH v/v, 98:2) to yield compounds **3** (5.8 mg) and **14** (2.5 mg). Fraction B2 was subjected to silica gel CC (CH_2Cl_2/MeOH v/v, 96:4) to yield compounds **9** (8.6 mg) and **13** (4.3 mg). Fraction C was eluted on Sephadex LH-20 CC (100% MeOH) to obtain compound **10** (7.5 mg) and two other fractions (Fr. C1–C2). Fraction C2 was separated using silica gel CC (CH_2Cl_2/MeOH v/v, 95:5) to yield compounds **11** (3.1 mg) and **12** (3.5 mg). Fraction D was eluted on Sephadex LH-20 CC (100% MeOH) to afford three fractions (Fr. D1–D3). Fraction D1 was purified by semipreparative UPLC (MeOH-H_2O, 7:3) to give compounds **1** (3.6 mg) and **2** (4.0 mg). Fraction D2 was subjected to silica gel CC (CH_2Cl_2/MeOH v/v, 9:1) to give compounds **4** (2.5 mg) and **7** (6.5 mg). Fraction E was subjected to Sephadex LH-20 CC (CH_2Cl_2/MeOH v/v, 1:1) to give compound **6** (3.8 mg) and another fraction E1. Compounds **5** (3.0 mg) and **8** (2.8 mg) were obtained from fraction E1, which was subjected to UPLC (MeOH-H_2O, 6:4).

"Fusarisetin E (**1**): Colorless oil, [α] + 10.0 (c = 0.16, MeOH). UV (MeOH) λ_{max} (log ε): 206 (3.02), 280 (2.16) nm. HRESIMS *m/*

TABLE 1 | ^{1}H and ^{13}C NMR data of compounds **1** and **2**.

No.	1			2		
	δ_C[a]	δ_H[a]	δ_H[b]	δ_C[a]	δ_H[a]	δ_Hb
1	65.1			65.3		
2	171.2			172.1		
3	68.9	3.16, dd (5.3, 6.8)	3.0, dd (4.2, 7.8)	68.6	4.0, dd (2.7, 7.4)	3.82, brd (8.5)
4	103.2			103.2		
5	76.8	4.37, qd (3.1, 6.9)	4.26, m	76.7	4.36, qd (3.2, 6.9)	4.23, m
6	46.2	2.59, dd (3.1, 11.9)	2.73, dd (3.6, 11.7)	45.1	2.59, dd (3.1, 11.9)	2.76, brd (9.5)
7	44.6	2.85, dd (4.7, 11.9)	2.44, dd (2.2, 11.9)	44.4	2.86, dd (4.6, 11.8)	2.44, dd (2.2, 12.0)
8	127.7	5.89, ddd (2.4, 4.8, 10.1)	5.84, brd (8.8)	127.7	5.88, ddd (2.4, 4.8, 10.1)	5.83, brd (8.8)
9	133.8	5.56, brd (10.1)	5.52, brd (10.1)	133.7	5.56, brd (10.1)	5.52, brd (9.8)
10	38.4	1.89, m	1.84, m	38.3	1.88, m	1.84, m
11	43.0	1.87, m	1.81, m	43.1	1.86, m	1.81, m
		0.82, q (12.7)	0.73, q (12.7)		0.82, q (12.7)	0.73, q (12.7)
12	34.1	1.49, m	1.41, m	34.1	1.49, m	1.41, m
13	36.5	1.75, m	1.70, m	36.4	1.75, m	1.70, m
		0.91, m	0.85, m		0.90, m	0.85, m
14	26.3	1.56, m	1.45, m	26.3	1.55, m	1.45, m
		1.0, m	1.04, m		1.0, m	1.04, m
15	40.0	1.37, m	1.18, m	39.8	1.37, m	1.18, m
16	53.2			53.1		
17	214.3			213.5		
18	62.6	4.07, dd (6.9, 11.7)	3.88, m	58.5	3.95, dd (2.8, 12.3)	3.87, brd (12.1)
		3.96, dd (5.3, 11.7)	3.78, dd (3.1, 11.0)		3.66, dd (7.4, 12.3)	3.38, m
19	30.5	3.03, s	2.92, s	28.6	3.02, s	2.88, s
20	17.7	1.34, d (7.0)	1.26, d (6.9)	17.4	1.33, d (7.0)	1.24, d (6.1)
21	22.7	0.93, d (6.5)	0.86, d (6.5)	22.7	0.93, d (6.5)	0.87, d (6.3)
22	15.0	1.0, s	0.89, s	14.7	1.0, s	0.91, s
OH-4				4.88, s		4.9, s
OH-18				7.3, s		7.5, s

[a]*Measured in* CD_3OD.
[b]*Measured in DMSO*-d_6.

TABLE 2 | ^{1}H and ^{13}C NMR data of compound **5** in $CDCl_3$.

5			5		
No.	δ_C	δ_H	**No.**	δ_C	δ_H
1	182.2		8	154.3	
2	114.7		8a	104.2	
3	162.9		9	9.2	2.02, s
4a	143.3		10	18.6	2.44, s
5	125.2		OCH_3-6	56.5	3.96, s
6	151.4		OH-5		5.14, s
7	94.5	6.41, s	OH-8		12.51, s

TABLE 3 | ^{1}H and ^{13}C NMR data of **9** and **10** in CD_3OD.

No.	9		10	
	δ_C	δ_H (*J* in Hz)	δ_C	δ_H (*J* in Hz)
2	169.4		163.5	
3	119.1		128.4	
3a	127.6		109.0	
4	98.9	7.02, d (2.2)	99.6	6.84, d (2.3)
5	139.1		137.2	
6	98.6	6.44, d (2.2)	97.3	6.27, d (2.3)
7	146.5		141.8	
7a	156.9		154.3	
8	12.7	2.75, s	13.1	2.70, s
9	187.4	10.14, s	166.3	
10	56.5	3.95, s		

z 406.22293 $[M + H]^+$ (calculated for $C_{22}H_{32}NO_6$ 406.22241). ^{1}H and ^{13}C NMR (CD_3OD-d_4) data, see **Table 1**.

Fusarisetin E (**2**): Colorless oil, [α] + 11.2 (c = 0.19, MeOH). UV (MeOH) λ_{max} (log ε): 204 (3.0), 282 (2.56) nm. HRESIMS *m/z* 406.22274 $[M + H]^+$ (calculated for $C_{22}H_{32}NO_6$ 406.22241). ^{1}H and ^{13}C NMR (CD_3OD-d_4) data, see **Table 1**.

Fusarimone A (**5**): Yellow solid. HRESIMS *m/z* 237.07583 $[M + H]^+$ (calculated for $C_{12}H_{13}O_5$ 237.07575). ^{1}H and ^{13}C NMR ($CDCl_3$) data, see **Table 2**.

Fusarifuran A (**9**): White solid, HRESIMS *m/z* 205.05090 [M-H]- (calculated for $C_{11}H_9O_4$ 205.05063). ^{1}H and ^{13}C NMR (CD_3OD-d_4) data, see **Table 3**.

Fusarifuran B (**10**): White solid, HRESIMS *m/z* 207.03026 $[M-H]^-$ (calculated for $C_{10}H_7O_5$ 207.02990). ^{1}H and ^{13}C NMR (CD_3OD-d_4) data, see **Table 3**.

Fusarimarin A (**11**): Colorless oil, [α] −21.5 (c 0.06, MeOH). UV (MeOH) λ_{max} (log ε): 219 (3.2), 238 (2.4), 318 (3.5) nm. HRESIMS *m/z* 279.12288 $[M + H]^+$ (calculated for $C_{15}H_{19}O_5$ 279.12270). ^{1}H and ^{13}C NMR ($CDCl_3$) data, see **Table 4**.

Fusarimarin B (**12**): Colorless oil, [α] +18.6 (c 0.07, MeOH). UV (MeOH) λ_{max} (log ε): 220 (3.3), 252 (3.0), 316 (3.4) nm.

TABLE 4 | ^{1}H and ^{13}C NMR data of **11–13** in $CDCl_3$.

No.	11		12		13	
	δ_C	δ_H (J in Hz)	δ_C	δ_H (J in Hz)	δ_C	δ_H (J in Hz)
1	166.2		166.6		164.8	
3	155.0		157.7		149.8	
4	106.1	6.29, s	104.3	6.19, s	111.8	6.60, s
4a	139.1		139.5		134.3	
5	101.4	6.33, d (2.2)	100.4	6.46, d (2.2)	103.6	6.49, brs
6	166.9		166.9		166.8	
7	100.5	6.48, d (2.2)	101.3	6.31, d (2.2)	102.1	6.58, brs
8	163.6		163.8		163.9	
8a	100.0		100.1		102.1	
9	41.6	2.69, dd (3.7, 14.6) 2.55, dd (8.6, 14.6)	33.3	2.53, t (2.5)	134.3	7.22, d (15.5)
10	68.9	4.07, m	23.2	1.83, m 1.73, m	122.5	6.68, d (15.5)
11	39.3	1.53, m	38.5	1.52, m	166.1	
12	18.7	1.51, m	67.9	3.84, m	61.0	4.29, dd (7.1, 14.1)
13	14.0	0.96, t (6.9)	23.9	1.22, d (6.2)	14.2	1.36, t (7.0)
OH-8		11.10, s		11.10, s		11.0, s
OCH_3-6	55.7	3.87, s	55.8	3.86, s	55.9	3.91, s

HRESIMS *m/z* 279.12290 $[M + H]^+$ (calculated for $C_{15}H_{19}O_5$ 279.12270). ^{1}H and ^{13}C NMR ($CDCl_3$) data, see **Table 4**.

Fusarimarin C (**13**): Colorless oil, HRESIMS *m/z* 291.08639 $[M + H]^+$ (calculated for $C_{15}H_{15}O_6$ 291.08631). ^{1}H and ^{13}C NMR ($CDCl_3$) data, see **Table 4**.

NMR Calculations

In general, conformational analysis was carried out using Merck Molecular Field by Spartan's 10 software. Conformers above 1% Boltzmann populations were optimized at the B3LYP/6-311+G (d, p) level in polarizable continuum model (PCM) methanol (Gaussian 09). Subsequently, NMR calculations were computed using the gauge invariant atomic orbital (GIAO) method at the mPWLPW91-SCRF/6-311+G (d, p) level using the PCM in methanol (Gaussian 09). Finally, the shielding constants were averaged by Boltzmann distribution theory for each stereoisomer, and their experimental and calculation data were analyzed by DP4+ probability.

ECD Calculations

The ECD calculations were performed as described previously (Chen et al., 2020). Geometric optimization of compounds **1** and **2** was carried out at the B3LYP/6-31+G(d) level in the liquid phase. Then, ECD calculations were performed using the TDDFT methodology at the WB97XD/CC-PVDZ and WB97XD/6-31G levels, respectively.

Cytotoxicity Assay

The cytotoxicity of all compounds against tumor cell lines was tested by the MTT assay as previously reported (Chen et al., 2019).

RESULTS AND DISCUSSION

Compound **1** was isolated as a colorless oil. The molecular formula was determined as $C_{22}H_{32}NO_6$ based on the HRESIMS data (*m/z* 406.22293 $[M + H]^+$). The ^{1}H NMR data of **1** (**Table 1**) showed three methyl signals at δ_H 0.93 (d, J = 6.5 Hz), 1.0 (s), and 1.34 (d, J = 7.0 Hz), one N-methyl proton at δ_H 3.03 (s), and two olefinic protons at δ_H 5.56 (brd, J = 10.1 Hz) and 5.89 (ddd, J = 2.4, 4.8, 10.1 Hz). The ^{13}C NMR data of **1** (**Table 1**) displayed 22 carbon signals, including four methyls, four methylenes (one oxygenated), seven methines (two olefinic), and four quaternary carbons (one ketone carbonyl and one ester carbonyl carbon). The planar structure of **1** was a detailed analysis of the 1D and 2D NMR data. The spin system of H_3-20/H-5/H-6/H-7/H-8/H-9/H-10/H_2-11/H-12(/H_3-21)/H_2-13/H_2-14/H-15(/H-10) from ^{1}H-^{1}H COSY data (**Figure 2**), together with the heteronuclear multiple-bond correlations (HMBC) (**Figure 2**) from H_3-22 to C-7, C-15, C-16 and C-17 and from H-6 to C-1, established the partial ring system of A/B/C, while the HMBC correlations from H-6 to C-2 and C-4, from H-3 to C-1 and C-4, and from H_3-19 to C-2 and C-3 indicated the presence of a γ-lactam moiety (ring D). In addition, a peroxide bridge between C-4 and C-5 was proposed according to two additional oxygen atoms in the molecular formula of **1**, which constitute the ring E. Thus, the planar structure of **1** was deduced (**Figure 1**), which was similar to fusarisetin A (Jang et al., 2011), by comparing their NMR data.

Compound **2**, with a molecular formula of $C_{22}H_{32}NO_6$, the same as **1**, was isolated as a colorless oil. The results of comparing the NMR data of **1** and **2** indicated that they shared a planar structure, and this was further confirmed by an extensive analysis of ^{1}H-^{1}H COSY and HMBC correlations (**Figure 2**), while the major difference of NMR shifts at H-3 ($\Delta\delta_H$ +0.84), C-18 ($\Delta\delta_C$ −4.1), and C-19 ($\Delta\delta_C$ −1.9) suggested **1** and **2** to be 3-epimers.

The relative configurations of **1** and **2** were determined by the NOESY correlations (**Figure 3**). The cross-peaks of H-12/H-10/H_3-22/H-7/H_3-20 suggested that these protons were co-facial, while the correlations of H_3-21/H-15/H-6 showed that these protons were on the other face. Considering the absence of

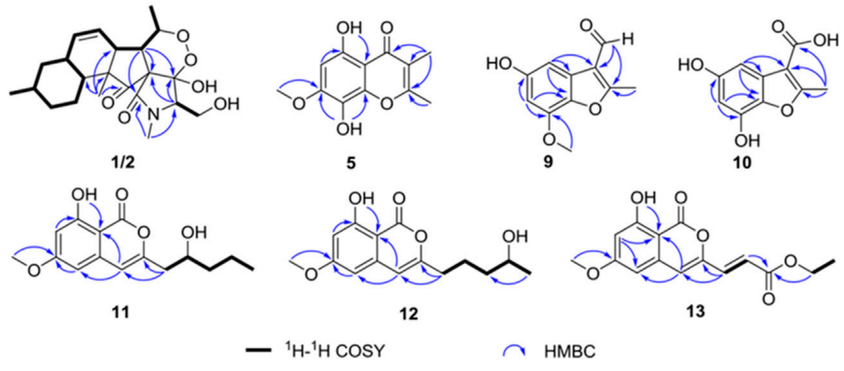

FIGURE 2 | Key heteronuclear multiple-bond correlations and correlation spectroscopy of compounds **1**, **2**, **5** and **9–13**.

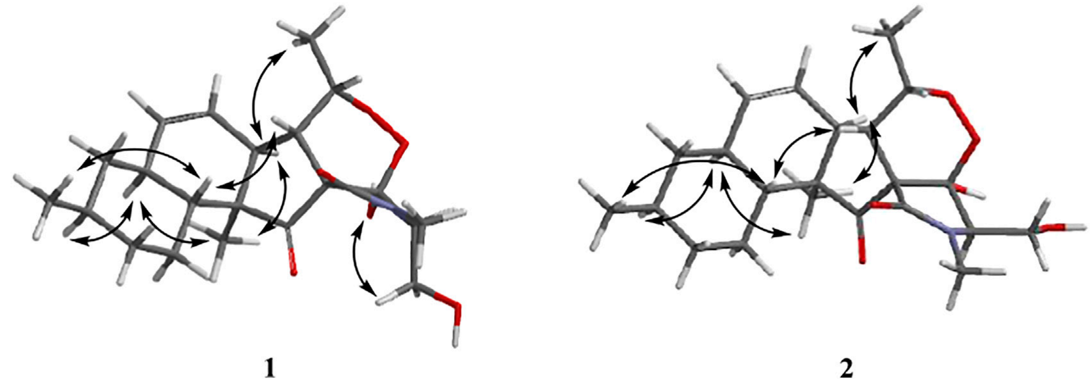

FIGURE 3 | Key nuclear Overhauser effect correlations of compounds **1** and **2**.

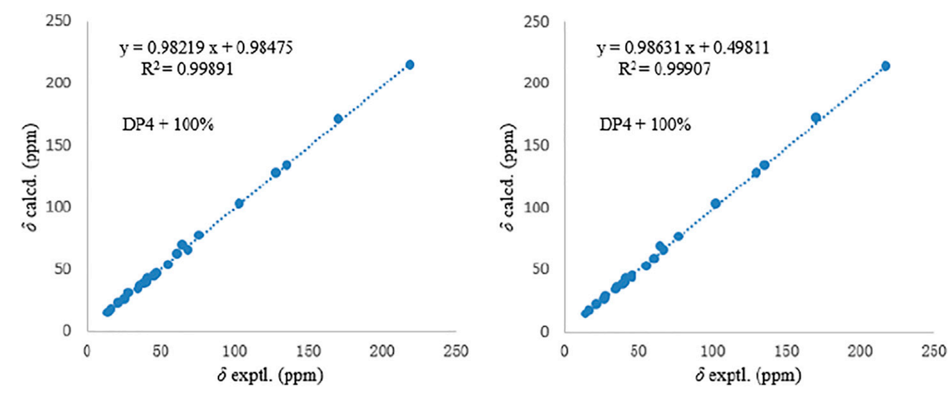

FIGURE 4 | Comparisons of calculated and experimental ^{13}C NMR data of **1** and **2**.

correlation from H_2-18 and 4-OH to other protons, the NOESY spectrum of **1** and **2** were retested in DMSO-d_6 reagent. Then, the correlation of 4-OH/H_2-18 was only detected in **1**, indicating that the protons of OH-4 and H_2-18 were positioned on the same face in **1** and were opposite in **2**. Thus, **1** and **2** were an epimer at C-3. Subsequently, the ^{13}C NMR calculations of (1*R**, 3*S**, 4*R**, 5*S**, 6*S**, 7*S**, 10*S**, 21*R**, 15*R**, 16*S**)-**1a** and (1*R**, 3*R**, 4*S**, 5*S**, 6*S**, 7*S**, 10*S**, 21*R**, 15*R**, 16*S**)-**1b** were carried out using the GIAO method at mPW1PW91-SCRF/6–311+G (d, p)/PCM (MeOH). The results of the DP4+ probability analysis (Smith and Goodman, 2010; Kawazoe et al., 2020; Xu et al., 2021) showed that **1a** was the most likely candidate structure, with a better correlation coefficient (R^2 = 0.99891) and a high DP4+ probability of 100% (all data) probability (**Figure 4**). Similarly,

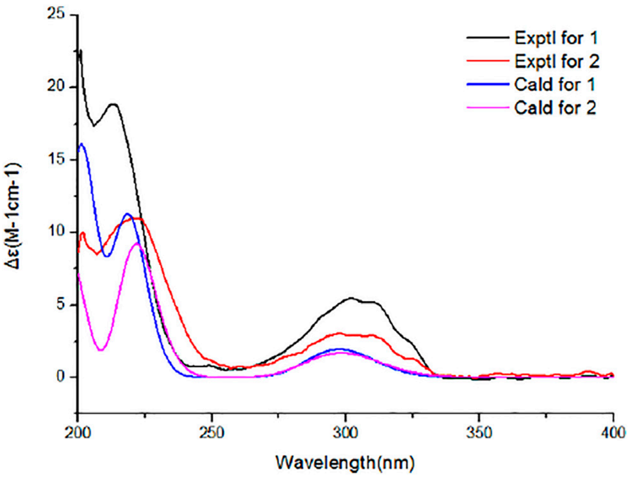

FIGURE 5 | Calculated and experimental electronic circular dichroism spectra of **1** and **2**.

^{13}C NMR calculations with the DP4+ probability analysis of the two isomers [(1*R**, 3*S**, 4*S**, 5*S**, 6*S**, 7*S**, 10*S**, 21*R**, 15*R**, 16*S**)-**2a** and (1*R**, 3*R**, 4*R**, 5*S**, 6*S**, 7*S**, 10*S**, 21*R**, 15*R**, 16*S**)-**2b**] of **2** were performed. The results showed that **2** gave the best match of 100% (all data) with the **2b** isomer.

Aiming at determining the absolute configuration of **1**, the ECD calculation was performed at the WB97XD/CC-PVDZ level. The results showed that the calculated ECD curve was in good agreement with the experimental one (**Figure 5**). Therefore, the absolute configuration of **1** was assigned as 1*R*, 3*S*, 4*R*, 5*S*, 6*S*, 7*S*, 10*S*, 21*R*, 15*R*, 16*S*. The absolute configuration of **2** was determined to be 1*R*, 3*R*, 4*R*, 5S, 6*S*, 7*S*, 10*S*, 21*R*, 15*R*, 16*S* by the identical experimental and calculated curves (**Figure 5**).

Compound **5** was obtained as a yellow solid. The molecular formula was determined to be $C_{12}H_{13}O_5$ based on HRESIMS data (*m/z* 237.07583 $[M + H]^+$). The ^{1}H NMR spectrum (**Table 2**) of **5** showed two methyl groups at δ_H 2.02 (s), 2.44 (s), one methoxyl group at δ_H 3.96 (s), one olefinic proton at δ_H 6.41 (s), and one chelated hydroxyl group at δ_H 12.51 (s). The ^{13}C NMR data (**Table 2**) of **5** highlighted the presence of 12 carbon resonances, including three methyls (one oxygenated), one olefinic carbon, and eight quaternary carbons (one carbonyl carbon and seven olefinic carbons). The ^{1}H and ^{13}C NMR data of **5** were similar to those of **6**, indicating that **5** was one chromone. The structure of **5** was further established by the HMBC correlations (**Figure 2**) from H_3-9 to C-1, C-2, and C-3 and from H_3-10 to C-3.

Compound **9** was obtained as a white solid. The molecular formula was determined to be $C_{11}H_9O_4$ based on HRESIMS data. The ^{1}H NMR spectrum (**Table 3**) of **9** showed one methyl group at δ_H 2.75 (s), one methoxyl group at δ_H 3.95 (s), and two aromatic protons at δ_H 7.02 (d, *J* = 2.2 Hz),6.44 (d, *J* = 2.2 Hz). The ^{13}C NMR data (**Table 3**) of **9** highlighted the presence of 11 carbon resonances, including two methyls, two sp^2 methines, and seven quaternary carbons. These data suggest **9** to be a benzofuran derivate. The NMR data of **9** were closely similar to penicifuran C (Qi et al., 2013), except for the presence of a methoxyl group, The HMBC correlations (**Figure 2**) from H_3-10 to C-7 indicated that the methoxyl group was located at C-7. Thus, the structure of **9** was determined as shown in **Figure 1**.

Compound **10** was obtained as a white solid. The molecular formula was determined to be $C_{10}H_{13}O_5$ based on HRESIMS data. The ^{1}H and ^{13}C NMR data (**Table 3**) of **10** were similar to those of **9**, except that the aldehyde group in **9** was oxidized to the carboxyl group, and there was an absence of the methoxyl group. The deduction was further confirmed by the HMBC correlations (**Figure 2**) from H_3-8 to C-2, C-3, and C-9. Therefore, the structure of **10** was established as shown.

Compound **11** had the molecular formula of $C_{15}H_{18}O_5$ by the HRESIMS data. The ^{1}H NMR spectrum (**Table 4**) of **11** showed one chelated hydroxyl group at δ_H 11.10 (s), one methyl group at δ_H 0.96 (t, *J* = 6.9 Hz), one methoxyl group at δ_H 3.87 (s), and three olefinic protons at δ_H 6.29 (s), 6.33 (d, *J* = 2.2 Hz), and 6.48 (d, *J* = 2.2 Hz). The ^{13}C NMR data (**Table 4**) of **11** revealed the presence of 15 carbon resonances, including two methyls, three methylenes, one sp^3 and three sp^2 methines, and six quaternary carbons. These data suggest **11** to be an isocoumarin class. The spin system of H_2-9/H-10/H_2-11/H_2-12/H_3-13 in the ^{1}H-^{1}H COSY spectrum (**Figure 2**) as well as the HMBC correlations (**Figure 2**) from H_2-9 to C-3 and C-4 showed that the side chain was substituted at C-3. By comparing the specific rotation of **11** [[α]−21.5 (c 0.06, MeOH)] with (−)-citreoisocoumarin [[α] −29.8 (c 0.34, MeOH)] (Mallampudi et al., 2020), the 10*R* configuration at C-10 in **11** was indicated. Thus, the gross structure of **11** was defined as shown.

Compound **12** was isolated as a colorless oil. The molecular formula was determined to be $C_{15}H_{18}O_5$ based on HRESIMS data. The comparison of the ^{1}H and ^{13}C NMR data (**Table 4**) with those of **11** revealed that they share the same isocoumarin structure, except that the hydroxyl group was substituted at C-12 in 12. The spin system of H_2-9/H_2-10/H_2-11/H-12/H_2-13 in the ^{1}H-^{1}H COSY spectrum (**Figure 2**), together with the HMBC correlations (**Figure 2**) from H_2-9 to C-3 and C-4, further supported this possibility. The 12*S* configuration was confirmed by the positive specific rotation value of **12** [[α] +18.6 (c 0.07, MeOH)] when compared with peneciraistin D [[α] +21.1 (c 0.14, MeOH)] (Ma et al., 2012).

Compound **13** was isolated as a colorless oil with the molecular formula of $C_{15}H_{14}O_6$ based on HRESIMS data. Upon comparing the ^{1}H and ^{13}C NMR data (**Table 4**) between **11** and **13**, it was suggested that **13** also possessed the isocoumarin framework. The spin system of H-9/H-10 observed in the ^{1}H-^{1}H COSY spectrum (**Figure 2**) and the HMBC correlations (**Figure 2**) from H-9 to C-3 and C-4 from H-10 to C-11 made it possible to obtain the gross structure. Additionally, an ethyl group was linked with C-11 by the HMBC correlations from H-12 to C-11. The 9*E* configuration of the double bond was determined by the large coupling constant $J_{H\text{-}9,\,H\text{-}10}$ = 15.5 Hz. Thus, the structure of **13** was confirmed as shown in **Figure 1**.

Five known analogues were characterized as equisetin (**3**) (Zhao et al., 2019), epi-equisetin (**4**) (Zhao et al., 2019), takanechromone B (**6**) (Qader et al., 2021), altechromone A (**7**) (Tanaka et al., 2009), 4H-1-benzopyran-4-one- 2,3-dihydro-5-hydroxy-8-(hydroxylmethyl)-2-methyl (**8**) (Sousa et al., 2016), and aspergisocoumrin A (**14**) (Wu

TABLE 5 | Cytotoxicity of compounds **1–4**, **8** and **13** (IC_{50} ± SD, μM).

Compound	A549	HELA	KYSE150	PC-3	MDA-MB-435
1	8.7 ± 0.6	39.2 ± 0.7	36.3 ± 0.5	>50	>50
2	4.3 ± 0.2	>50	>50	>50	>50
4	15.3 ± 0.6	>50	>50	>50	>50
8	5.6 ± 1.3	>50	>50	>50	3.8 ± 0.3
13	>50	>50	>50	>50	30.5 ± 0.1
14	6.2 ± 0.2	—	—	—	2.8 ± 0.8
DDP[a]	25.9 ± 0.8	10.0 ± 0.1	72.6 ± 4.3	41.6 ± 0.9	9.6 ± 0.9

[a]*Positive control. "—" not tested.The IC_{50} values were expressed as means ± SD (n = 3) from three independent experiments.*

et al., 2019) through a comparison of the spectroscopic data with the literature.

All compounds were evaluated for their cytotoxicity against the A549 (lung carcinoma), HELA (cervical carcinoma), KYSE150 (esophageal squamous carcinoma), PC-3 (pancreatic carcinoma), and MDA-MB-435 (breast carcinoma) human cancer cell lines (**Table 5**). As a result, compounds **1** and **2** showed selective cytotoxicity against A549 cell line with IC_{50} values of 8.7 and 4.3 μM, respectively. Compound **8** showed potent cytotoxicity against A549 and MDA-MB-435 cell lines with IC_{50} values of 5.6 and 3.8 μM, respectively. Compound **14** exhibited significant cytotoxicity against A549 and MDA-MB-435 cell lines with IC_{50} values of 6.2 and 2.8 μM, respectively, while the other compounds exhibited non-significant activity against the five cancer cell lines at the concentration of 50 μM.

CONCLUSION

In summary, two new 3-decalinoyltetramic acid (3DTA) derivatives, fusarisetins E (**1**) and F (**2**), with a peroxide bridge, were isolated from mangrove endophytic fungus *Fusarium* sp. 2ST2. The 3DTA derivatives showed various bioactivities, such as antimicrobial, anticancer, larvicidal, cytotoxic, and antiviral (Fan et al., 2020). The structure of fusarisetins E (**1**) and F (**2**) was similar to that of fusarisetin A, which was first isolated from the soil fungus *Fusarium* sp. FN080326 with inhibitory activity to acinar morphogenesis (Jang et al., 2011), while fusarisetin E (**1**) was identified as peroxyfusarisetin (Yin et al., 2012), a synthetic intermediate by mixture. Here fusarisetin E (**1**) was reported first as an optically pure new natural product with 1D and 2D NMR data (**Supplementary Figures S1–S8**). Moreover, natural peroxide compounds that usually have unique pharmacological activities, such as artemisinin with antimalarial activity (Zhao et al., 2018; Pandey et al., 1999), talaperoxides A-D with cytotoxicity (Li et al., 2011), phaeocaulisin M with anti-inflammatory activity (Ma et al., 2015), 1α,8α-epidioxy-4α-hydroxy-5αH-guai-7(11),9-dien-12,8-olide with antiviral activity (Dong et al., 2013), and plakinic acid M with antifungal activity (Matthew et al., 2016), were reported. Compounds **1** and **2** had selective cytotoxicity against A549 cell line with IC_{50} values of 8.7 and 4.38 μM, respectively. The cytotoxicity of fusarisetins was reported for the first time.

DATA AVAILABILITY STATEMENT

The original contributions presented in the study are included in the article/**Supplementary Material**, further inquiries can be directed to the corresponding authors.

AUTHOR CONTRIBUTIONS

YC performed the experiments, analyzed the data, and wrote the paper. GW and YY completed the biological activity test. GZ, WY, and QT participated in the experiments (fermentation and extraction of the strain). WK and ZS reviewed the manuscript. ZS designed and supervised the experiments. All authors have read and agreed to the published version of the manuscript.

FUNDING

This research received generous support and was funded by the National Natural Science Foundation of China (U20A2001, 21877133), Development Program of Guangdong Province (2020B1111030005), Key Project in Science and Technology Agency of Henan Province (212102311029), and Key Scientific Research Project in Colleges and Universities of Henan Province (22B350001).

SUPPLEMENTARY MATERIAL

The Supplementary Material for this article can be found online at: https://www.frontiersin.org/articles/10.3389/fchem.2022.842405/full#supplementary-material

REFERENCES

Cai, R., Jiang, H., Xiao, Z., Cao, W., Yan, T., Liu, Z., et al. (2019). (−)- and (+)-Asperginulin A, a Pair of Indole Diketopiperazine Alkaloid Dimers with a 6/5/4/5/6 Pentacyclic Skeleton from the Mangrove Endophytic Fungus Aspergillus Sp. SK-28. *Org. Lett.* 21, 9633–9636. doi:10.1021/acs.orglett.9b03796

Chen, J., Bai, X., Hua, Y., Zhang, H., and Wang, H. (2019a). Fusariumins C and D, Two Novel Antimicrobial Agents from *Fusarium Oxysporum* ZZP-R1

Symbiotic on Rumex Madaio Makino. *Fitoterapia* 134, 1–4. doi:10.1016/j.fitote.2019.01.016

Chen, S., Cai, R., Liu, Z., Cui, H., and She, Z. (2022). Secondary Metabolites from Mangrove-Associated Fungi: Source, Chemistry and Bioactivities. *Nat. Prod. Rep.* doi:10.1039/D1NP00041A

Chen, Y., Liu, Z., Huang, Y., Liu, L., He, J., Wang, L., et al. (2019b). Ascomylactams A-C, Cytotoxic 12- or 13-Membered-Ring Macrocyclic Alkaloids Isolated from the Mangrove Endophytic Fungus *Didymella* Sp. CYSK-4, and Structure Revisions of Phomapyrrolidones A and C. *J. Nat. Prod.* 82, 1752–1758. doi:10.1021/acs.jnatprod.8b00918

Chen, Y., Zhang, L., Zou, G., Li, C., Yang, W., Liu, H., et al. (2020). Anti-inflammatory Activities of Alkaloids from the Mangrove Endophytic Fungus *Phomopsis* Sp. SYSUQYP-23. *Bioorg. Chem.* 97, 103712. doi:10.1016/j.bioorg.2020.103712

Chen, Y., Zou, G., Yang, W., Zhao, Y., Tan, Q., Chen, L., et al. (2021). Metabolites with Anti-inflammatory Activity from the Mangrove Endophytic Fungus Diaporthe Sp. QYM12. *Mar. Drugs* 19, 56. doi:10.3390/md19020056

Cui, H., Lin, Y., Luo, M., Lu, Y., Huang, X., and She, Z. (2017). Diaporisoindoles A-C: Three Isoprenylisoindole Alkaloid Derivatives from the Mangrove Endophytic Fungus Diaporthe Sp. SYSU-HQ3. *Org. Lett.* 19, 5621–5624. doi:10.1021/acs.orglett.7b02748

Dong, J.-Y., Ma, X.-Y., Cai, X.-Q., Yan, P.-C., Yue, L., Lin, C., et al. (2013). Sesquiterpenoids from *Curcuma Wenyujin* with Anti-influenza Viral Activities. *Phytochemistry* 85, 122–128. doi:10.1016/j.phytochem.2012.09.008

Fan, B., Dewapriya, P., Li, F., Grauso, L., Blümel, M., Mangoni, A., et al. (2020). Pyrenosetin D, a New Pentacyclic Decalinoyltetramic Acid Derivative from the Algicolous Fungus Pyrenochaetopsis Sp. FVE-087. *Mar. Drugs* 18, 281. doi:10.3390/md18060281

Guo, Y.-W., Liu, X.-J., Yuan, J., Li, H.-J., Mahmud, T., Hong, M.-J., et al. (2020). l-Tryptophan Induces a Marine-Derived *Fusarium* Sp. To Produce Indole Alkaloids with Activity against the Zika Virus. *J. Nat. Prod.* 83, 3372–3380. doi:10.1021/acs.jnatprod.0c00717

Huang, X., Huang, H., Li, H., Sun, X., Huang, H., Lu, Y., et al. (2013). Asperterpenoid A, a New Sesterterpenoid as an Inhibitor of Mycobacterium tuberculosis Protein Tyrosine Phosphatase B from the Culture of Aspergillus Sp. 16-5c. *Org. Lett.* 15, 721–723. doi:10.1021/ol303549c

Ibrahim, S. R. M., Mohamed, G. A., Al Haidari, R. A., Zayed, M. F., El-Kholy, A. A., Elkhayat, E. S., et al. (2018). Fusarithioamide B, a New Benzamide Derivative from the Endophytic Fungus *Fusarium Chlamydosporium* with Potent Cytotoxic and Antimicrobial Activities. *Bioorg. Med. Chem.* 26, 786–790. doi:10.1016/j.bmc.2017.12.049

Jang, J.-H., Asami, Y., Jang, J.-P., Kim, S.-O., Moon, D. O., Shin, K.-S., et al. (2011). Fusarisetin A, an Acinar Morphogenesis Inhibitor from a Soil Fungus, Fusarium Sp. FN080326. *J. Am. Chem. Soc.* 133, 6865–6867. doi:10.1021/ja1110688

Kawazoe, R., Matsuo, Y., Saito, Y., and Tanaka, T. (2020). Computationally Assisted Structural Revision of Flavoalkaloids with a Seven-Membered Ring: Aquiledine, Isoaquiledine, and Cheliensisine. *J. Nat. Prod.* 83, 3347–3353. doi:10.1021/acs.jnatprod.0c00691

Li, H., Huang, H., Shao, C., Huang, H., Jiang, J., Zhu, X., et al. (2011). Cytotoxic Norsesquiterpene Peroxides from the Endophytic Fungus *Talaromyces flavus* Isolated from the Mangrove Plant *Sonneratia Apetala*. *J. Nat. Prod.* 74, 1230–1235. doi:10.1021/np200164k

Liu, G., Huo, R., Zhai, Y., and Liu, L. (2021). New Bioactive Sesquiterpeniods from the Plant Endophytic Fungus Pestalotiopsis theae. *Front. Microbiol.* 12, 641504. doi:10.3389/fmicb.2021.641504

Liu, Z., Chen, Y., Chen, S., Liu, Y., Lu, Y., Chen, D., et al. (2016). Aspterpenacids A and B, Two Sesterterpenoids from a Mangrove Endophytic Fungus *Aspergillus terreus* H010. *Org. Lett.* 18, 1406–1409. doi:10.1021/acs.orglett.6b00336

Ma, J.-H., Wang, Y., Liu, Y., Gao, S.-Y., Ding, L.-Q., Zhao, F., et al. (2015). Four New Sesquiterpenes from the Rhizomes ofCurcuma Phaeocaulisand Their iNOS Inhibitory Activities. *J. Asian Nat. Prod. Res.* 17, 532–540. doi:10.1080/10286020.2015.1046449

Ma, L.-Y., Liu, W.-Z., Shen, L., Huang, Y.-L., Rong, X.-G., Xu, Y.-Y., et al. (2012). Spiroketals, Isocoumarin, and Indoleformic Acid Derivatives from saline Soil Derived Fungus *Penicillium raistrickii*. *Tetrahedron* 68, 2276–2282. doi:10.1016/j.tet.2012.01.054

Mallampudi, N. A., Choudhury, U. M., and Mohapatra, D. K. (2020). Total Synthesis of (−)-Citreoisocoumarin, (−)-Citreoisocoumarinol, (−)-12-Epi-Citreoisocoumarinol, and (−)-Mucorisocoumarins A and B Using a Gold(I)-Catalyzed Cyclization Strategy. *J. Org. Chem.* 85, 4122–4129. doi:10.1021/acs.joc.9b03278

Matthew, T. J., Doralyn, S. D., and Tadeusz, F. M. (2016). Peroxide Natural Products from *Plakortis Zyggompha* and the Sponge Association *Plakortis Halichondrioides-Xestospongia Deweerdtae*: Antifungal Activity against *Cryptococcus Gattii*. *J. Nat. Prod.* 79, 555. doi:10.1021/acs.jnatprod.5b00951

Pandey, A. V., Tekwani, B. L., Singh, R. L., and Chauhan, V. S. (1999). Artemisinin, an Endoperoxide Antimalarial, Disrupts the Hemoglobin Catabolism and Heme Detoxification Systems in Malarial Parasite. *J. Biol. Chem.* 274, 19383–19388. doi:10.1074/jbc.274.27.19383

Qader, M. M., Hamed, A. A., Soldatou, S., Abdelraof, M., Elawady, M. E., Hassane, A. S. I., et al. (2021). Antimicrobial and Antibiofilm Activities of the Fungal Metabolites Isolated from the Marine Endophytes *Epicoccum Nigrum* M13 and *Alternaria alternata* 13A. *Mar. Drugs* 19, 232. doi:10.3390/md19040232

Qi, J., Shao, C.-L., Li, Z.-Y., Gan, L.-S., Fu, X.-M., Bian, W.-T., et al. (2013). Isocoumarin Derivatives and Benzofurans from a Sponge-Derived *Penicillium* Sp. Fungus. *J. Nat. Prod.* 76, 571–579. doi:10.1021/np3007556

Smith, S. G., and Goodman, J. M. (2010). Assigning Stereochemistry to Single Diastereoisomers by GIAO NMR Calculation: the DP4 Probability. *J. Am. Chem. Soc.* 132, 12946–12959. doi:10.1021/ja105035r

Sousa, J. P. B., Aguilar-Pérez, M. M., Arnold, A. E., Rios, N., Coley, P. D., Kursar, T. A., et al. (2016). Chemical Constituents and Their Antibacterial Activity from the Tropical Endophytic Fungus *Diaporthe* Sp. F2934. *J. Appl. Microbiol.* 120, 1501–1508. doi:10.1111/jam.13132

Tanaka, N., Kashiwada, Y., Nakano, T., Shibata, H., Higuchi, T., Sekiya, M., et al. (2009). Chromone and Chromanone Glucosides from *Hypericum Sikokumontanum* and Their Anti-Helicobacter pylori Activities. *Phytochemistry* 70, 141–146. doi:10.1016/j.phytochem.2008.11.006

Viridiana, M. S., Carmen, E. D., Olmeda, SA, Valcarcel, F, Elena, T., Azucena, G. C., et al. (2021). Bioactive Metabolites from the Endophytic Fungus *Aspergillus* Sp. SPH2. *J. Fungi* 7, 109. doi:10.3390/md13053091

Wu, Y., Chen, S., Liu, H., Huang, X., Liu, Y., Tao, Y., et al. (2019). Cytotoxic Isocoumarin Derivatives from the Mangrove Endophytic Fungus *Aspergillus* Sp. HN15-5D. *Arch. Pharm. Res.* 42, 326–331. doi:10.1007/s12272-018-1019-1

Xiao, Z. e., Huang, H., Shao, C., Xia, X., Ma, L., Huang, X., et al. (2013). Asperterpenols A and B, New Sesterterpenoids Isolated from a Mangrove Endophytic Fungus Aspergillus Sp. 085242. *Org. Lett.* 15, 2522–2525. doi:10.1021/ol401005j

Xu, M.-M., Zhou, J., Zeng, L., Xu, J., Onakpa, M. M., Duan, J.-A., et al. (2021). Pimarane-derived Diterpenoids with Anti-Helicobacter pylori Activity from the Tuber of Icacina Trichantha. *Org. Chem. Front.* 8, 3014–3022. doi:10.1039/d1qo00374g

Yin, J., Wang, C., Kong, L., Cai, S., and Gao, S. (2012). Asymmetric Synthesis and Biosynthetic Implications of (+)-Fusarisetin A. *Angew. Chem. Int. Ed.* 51, 7786–7789. doi:10.1002/anie.201202455

Zhao, D., Han, X., Wang, D., Liu, M., Gou, J., Peng, Y., et al. (2019). Bioactive 3-Decalinoyltetramic Acids Derivatives from a Marine-Derived Strain of the Fungus *Fusarium Equiseti* D39. *Front. Microbiol.* 10, 1285. doi:10.3389/fmicb.2019.01285

Zhao, Q., Gao, J.-J., Qin, X.-J., Hao, X.-J., He, H.-P., and Liu, H.-Y. (2018). Hedychins A and B, 6,7-Dinorlabdane Diterpenoids with a Peroxide Bridge from Hedychium Forrestii. *Org. Lett.* 20, 704–707. doi:10.1021/acs.orglett.7b03836

Conflict of Interest: The authors declare that the research was conducted in the absence of any commercial or financial relationships that could be construed as a potential conflict of interest.

Publisher's Note: All claims expressed in this article are solely those of the authors and do not necessarily represent those of their affiliated organizations or those of the publisher, the editors, and the reviewers. Any product that may be evaluated in this article or claim that may be made by its manufacturer is not guaranteed or endorsed by the publisher.

Copyright © 2022 Chen, Wang, Yuan, Zou, Yang, Tan, Kang and She. This is an open-access article distributed under the terms of the Creative Commons Attribution License (CC BY). The use, distribution or reproduction in other forums is permitted, provided the original author(s) and the copyright owner(s) are credited and that the original publication in this journal is cited, in accordance with accepted academic practice. No use, distribution or reproduction is permitted which does not comply with these terms.